

CONCENTRATOR EFFECT OF BUILDINGS ON THE ENERGY PRODUCTION OF HORIZONTAL AXIS WIND TURBINES (HAWTS)

Victor Manuel Padilla Segura

UIDET-LaCLyFA, Departamento
Aeronáutica, Facultad de
Ingeniería, Universidad Nacional de La Plata,
La Plata, Buenos Aires, Argentina

Julio Marañón Di Leo

UIDET-LaCLyFA, Departamento
Aeronáutica, Facultad de
Ingeniería, Universidad Nacional de La Plata,
La Plata, Buenos Aires, Argentina
CONICET, Ciudad. de Buenos Aires,
Argentina

Juan Sebastián delnero

UIDET-LaCLyFA, Departamento
Aeronáutica, Facultad de
Ingeniería, Universidad Nacional de La Plata,
La Plata, Buenos Aires, Argentina
CONICET, Ciudad. de Buenos Aires,
Argentina

Pablo Marcelo Mantelli

UIDET-LaCLyFA, Departamento
Aeronáutica, Facultad de
Ingeniería, Universidad Nacional de La Plata,
La Plata, Buenos Aires, Argentina

All content in this magazine is licensed under a Creative Commons Attribution License. Attribution-Non-Commercial-Non-Derivatives 4.0 International (CC BY-NC-ND 4.0).



Abstract: This paper describes wind tunnel measurements carried out to determine the advantages of the concentrator effect of buildings as a way to improve wind energy production in cities. Measurements of flow velocity were taken with the use of hot wire anemometry above the rooftop of a 15 storey 1:80 scaled generic shaped building. This flow was affected by another building located upstream, with variable height.

The measured data was analyzed to determine flow characteristics such as; velocity field, turbulence intensity, autocorrelation coefficients, RMS (root mean square) and PSD (power spectral density).

The experiments showed increases in velocity of between 21 and 43% above the building rooftop. This increase was found to be maximized when the flow above the building is not affected by surrounding buildings. Thus, potential advantages of the location of wind turbines on building terraces were demonstrated.

INTRODUCTION

Wind is a worldwide energy resource that has gained the attention of many researchers looking to harness its power. More specifically, concentration effects could significantly improve the wind mean velocity in relatively limited spaces. Such effects not only appear in nature, but also in urban areas, and thus the way they impact this renewable energy resource becomes of interest.

Buildings can accelerate the wind around them by over 20%. This energy boost can be an advantage to power produced through wind turbines adequately located above buildings. Thereby, the integration of wind turbines onto buildings becomes an advantageous possibility. The phenomenon is being studied in wind energy research groups around the world, like at the Technical University of Delft in the Netherlands. Also, studies have been

performed in other locations, like Amsterdam, La Haya, Tilburg and Twente and also in the United Kingdom [1].

Wang et al [2] studied the possibility of locating wind turbines on building rooftops. At the same time, Grant et al [3] considered locating vertical and horizontal axis wind turbines inside ducts near the edges of tall buildings terraces, where the wind pressure diminishes, creating a suction force. Lu and Ka Yan [4] performed computational fluid dynamics calculus (CFD calculus) with different groups of buildings. They found a velocity increase between 1.5 and 2 times the upstream wind mean velocity and, hence, an increased power between 3 and 8 times.

Mithraratne [5] evaluated the possibility of installing relatively small wind turbines on building rooftops in New Zealand. He concluded that by using such devices, the carbon dioxide emissions could be reduced between 26 and 81% in this country.

One example in Argentina is the Cefira tower in the city of Mardel Plata. A 4.5kW powered Horizontal Axis Wind Turbine (HAWT) is located on its terrace, capable of supplying 15% of the electricity consumed by the building [6].

The first building which integrated wind turbines into its structure was the Bahrain World Trade Center, built in 2006 (Alnaser et al [7]). The 240 m height building has two identical triangular towers, connected by three bridges, each one with a HAWT, creating a unique space to achieve enough wind to move the big turbine rotors. Wind turbines were located in a way to maximize wind velocity on the rotor planes, satisfying Bernoulli's principle, by forcing the same air volume to flow in a small space like a venturi tube. Wind tunnel experiments showed that if wind flow is perpendicular to the rotors, the energy production should be around 11% to 15% of the total building's energy consumption.

Another large scale building integrating wind turbines is the “Pearl River Tower”, located in the city of Guangzhou, China [8]. The 303 m height and 69 story building has a curved geometry. It was designed aerodynamically, with the aim of accelerating and redirecting the wind into a four wind turbine system, located at two different heights of the building.

Muller et al [9] analyzed primitive devices for converting wind energy into electricity: the Giromill and the Savonius. Also, they studied the modern adaptations of such devices for their integration into building design. These studies showed the possibility of theoretical efficiency from 48% (conservative) to 61% (optimistic). They performed experiments with a scale model and showed that the highest efficiency attainable was 40%, that is, less than the predicted theoretical conservative value.

At the moment, the Architecture firm Waugh Thistleton [10] has developed a new project, consisting of incorporating HAWTs into an existing 14 story building, located just east of London. In this way, the building itself could be capable of producing about 15% of its energy requirements, representing about 40,000 kWh per year.

In this study, an experimental approach is developed. Measurements of flow velocity were taken above the rooftop of a 15 storey 1:80 scaled generic-shaped building. This was performed using the method of hot wire anemometry in a boundary layer wind tunnel. The flow above the building was affected by another similar building, with variable height, situated upstream. Then the collected data permitted characterization of the flow above the building, determining parameters such as; velocity field, turbulence intensity, autocorrelation coefficients, RMS (root mean square) and PSD (power spectral density). With the characterization of the

flow permitted to find conclusions about the location and characteristics of HAWTs in the built environment, such as the tower's height and its close relation with the location of the systems.

METHODOLOGY

SCALE BUILDING MODEL

Two models of a 20 story 1:80 scaled generic shape building were built (“Building A” and “Building B”). Each one represented a real building with a height of 56m. The Building A model was integrated with five separated modules, the first one with a height of 30 cm, and the remaining four with 10 cm each. This was made with the purpose of varying the height of Building A. On the other hand, Building B had a fixed height of 70 cm. Both buildings had a squared base of 35 x 35 cm.

The models were made with laser cut wood. They were attached to a 0.05 x 1.21 x 0.65 m wooden board, which was subsequently bolted to the wind tunnel floor.

The wooden models were painted to protect them from moisture. As can be seen in Figure 4, the white stripes painted on the models represent an average height of two stories.

The models were separated by a distance of 0.21 m, or 17 minreal scale. This distance represents the average width of an avenue plus sidewalks, according to Argentine building codes.

FACILITIES AND FREE STREAM CHARACTERIZATION

The experiments were conducted at the University of La Plata's UIDET LaCLyFA's boundary layer wind tunnel, which has a nominal test section of 1.83 m height and 2.6 m width.

The velocity profile utilized for the tests

was a common atmospheric low boundary layer profile following the power law, with a surface roughness of 2 m. According to reference [11], this roughness corresponds to a terrain with high objects, as those of an urban environment.

The power law for velocity distribution is given by:

$$\frac{\bar{U}}{U_g} = \left(\frac{Z}{Z_g} \right)^\alpha$$

\bar{U} = Velocity at height Z .

U_g = Reference velocity = 10 m/s.

Z_g = Reference height = 50 m.

$\alpha = 0.16$.

- Geometric configurations

Three configurations of buildings were tested. The Building A height differed through the configurations, as shown in Figures 1, 2 and 3.

In configuration 1, Building A has a height of 24 m, while in configurations 2 and 3, it is of 40 m and 56 m, respectively.

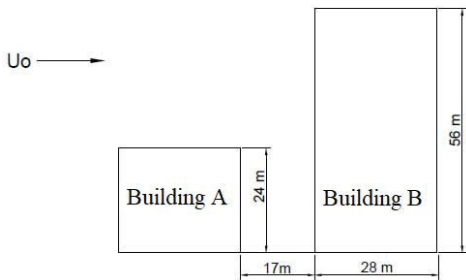


Figure 1: Configuration 1

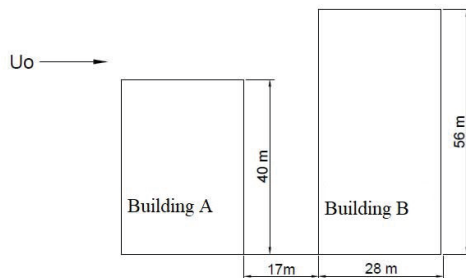


Figure 2: Configuration 2

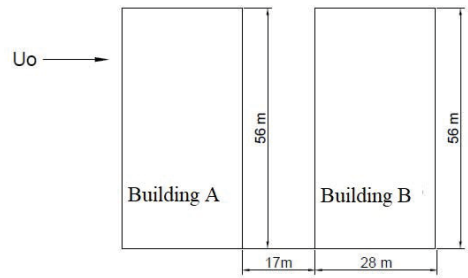


Figure 3: Configuration 3

In the figures above, U_0 represents the free flow direction.

- Flow visualization test

A test was made with the aim of visualizing the flow above the building rooftop. Based on this, it was possible to define the heights in which the measurements of velocity were made.

This test was conducted with the use of smoke as the element of visualization of flow. In that sense, a smoke generation machine was used. The flow velocity during the test was of 2 m/s, and a camera was used to record approximately 30 seconds of each test.

FLOW VELOCITY MEASUREMENTS ABOVE THE ROOFTOP

The test consisted in the measurement of flow velocities above the Building B rooftop, with the aim of determining the velocity field. For this purpose, a 9 points grid on the rooftop was utilized, as can be seen in Figure 4. On each of these points velocities were measured at heights of; 5, 10, 15, 20 and 25 cm.

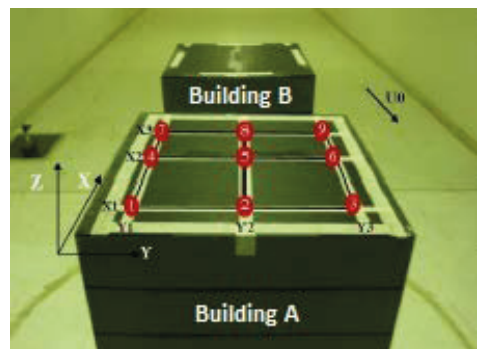


Figure 4: measurement points grid

The velocities were measured using hot-wire anemometry. This was done with the use of the DANTEC Streamline data acquisition system and a DANTEC hot wire probe.

The probe was mounted on a metallic support attached to a carriage which was driven vertically on a track. In this way, it was possible to perform the measurements automatically at different heights above the building rooftop.

First, the probe was located above point 1 on the grid, at a height of 5 cm. Second, wind tunnel velocity was set to 10 m/sec and measurements were made. Then, the probe was moved to a height of 10 cm above the rooftop and again measurements were made. This process was repeated for heights of 15, 20 and 25 cm and for each of the remaining points of the grid. This procedure was replicated for the three different configurations of Building A.

The data was acquired at 2,000 Hz and over samples were collected for each measurement point.

RESULTS

A large amount of data was acquired and analyzed in the experiments, but only a small amount can be presented in this paper. The reader wishing to obtain more data can contact us for further information.

The results presented below correspond only to configurations 1 and 3, which proved to be the most advantageous in terms of velocity in crease and flow direction.

FLOW VISUALIZATION TEST

For configuration 1 it can be seen from Figure 5, that Building A does not affect the flow above the Building B rooftop. The flow seems unaffected by the presence of Building A, and it is observed that the pattern of flow above Building A is that of free flow.

At the same time, the flow above the Building B rooftop seems to recover its

original direction at a height of 12.2 cm or 9.8 m in real scale (this will be verified after the analysis of velocities), where it is observed to become parallel to the rooftop surface.

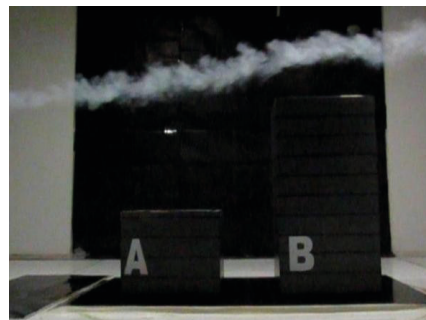


Figure 5: Smoke test for Configuration 1.

For configuration 3 it can be seen from Figure 6, that Building A affects the flow above the Building B rooftop. The flow seems to become more dispersed and parallel to the rooftop surface at a lower height compared to configuration 1.

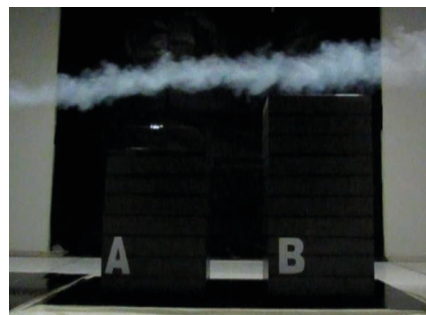


Figure 6: Smoke test for Configuration 3.

FLOW CHARACTERIZATION ABOVE THE ROOFTOP

The analysis described below refers only to the measurements made above the grid (Figure 4) points 2, 5 and 9. These points are included in the plane Y2-Z. Thus, hereinafter, every diagram will correspond to measurements made in this plane.

- Mean velocities

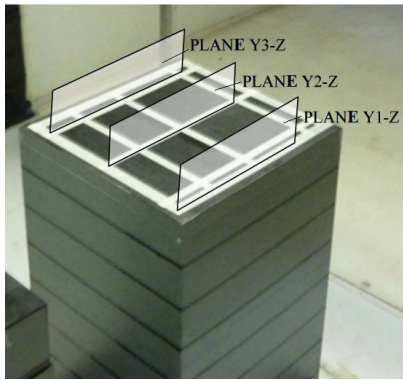


Figure 7: Planes of measurement

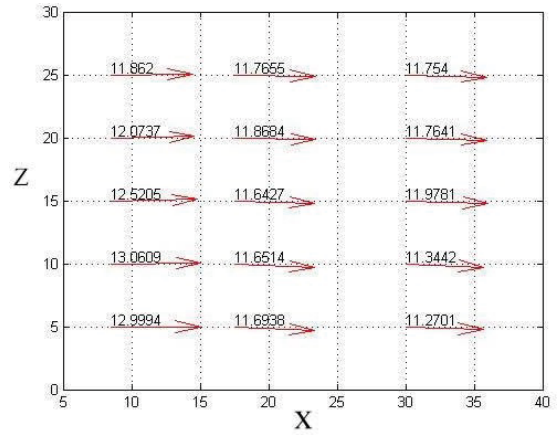


Figure 9: velocity field for configuration 3

The following diagrams show the velocity field for the plane Y2-Z and each configuration. The vectors indicate the coordinates of the measurement points, and the magnitude and direction of the velocity. The X axis coordinates correspond to the distance from the incidence edge of the rooftop in cm, and the Y axis coordinates correspond to the height from the rooftop surface in cm.

In configuration 3, the most remarkable phenomenon is that velocities remain similar for each measurement point. And in the same way, the flow, as seen in Figure 9, is almost parallel to the rooftop surface.

- Turbulence Intensity

The turbulence intensity values for both U and V velocity components, in blue and orange, respectively, are shown in the diagrams below. The results for configuration 1 above grid points 5 and 8 are the

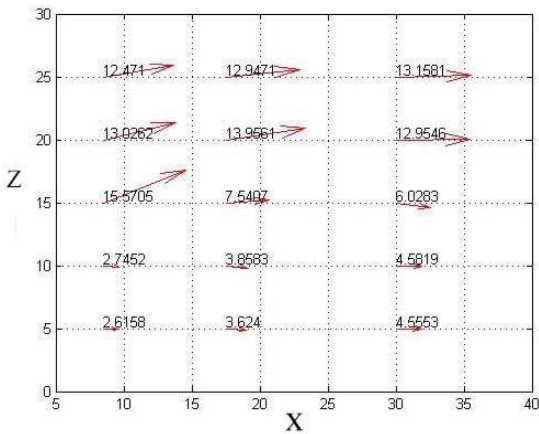


Figure 8: velocity field for configuration 1.

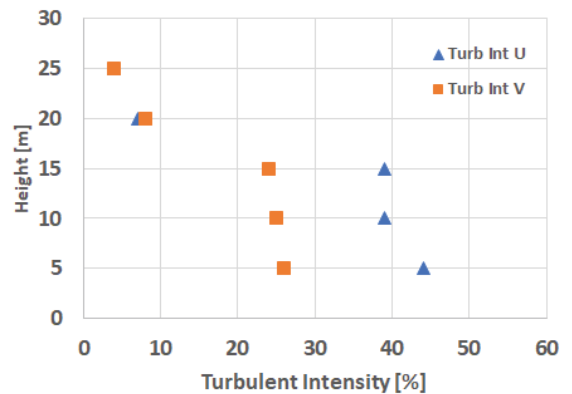


Figure 10: Configuration 1 turbulence intensity at point 5.

For configuration 1, a considerable increase in velocity at 15 cm of height can be seen. This is due to the effects of the high turbulence near the rooftop surface, which translates to low velocities. Also, the higher magnitudes take place near the incidence edge.

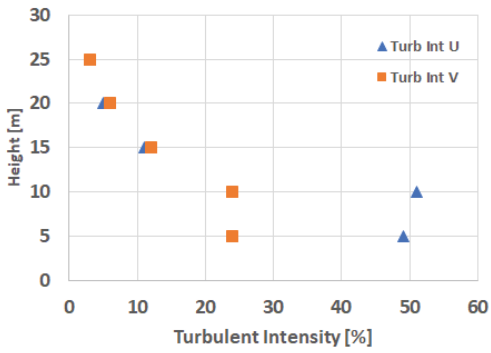


Figure 11: Configuration 1 turbulence intensity at point 8.

For point 5, above a 15 cm height, turbulence is reduced considerably, reducing from values above 45 m/s to values below 15 m/s, for the horizontal component of velocity. This phenomenon occurs above a 10 cm height for point 8, which is closer to the building edge.

The diagrams below correspond to configuration 3.

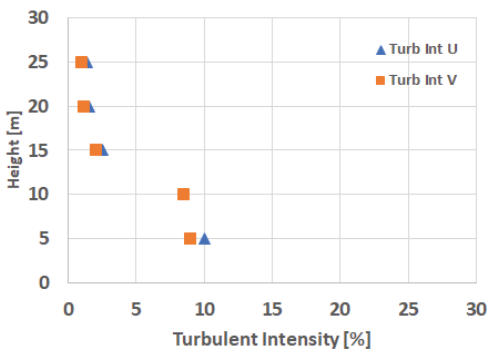


Figure 12: turbulence intensity in point 5 of Configuration 3.

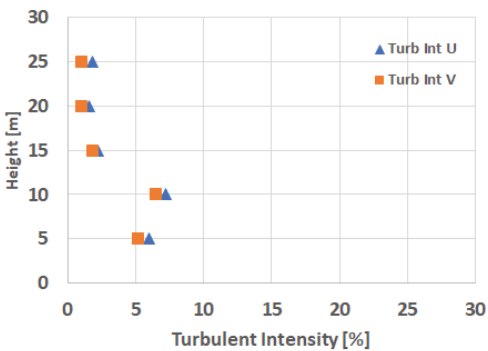


Figure 13: turbulence intensity in point 8 of Configuration 3.

This configuration follows the same behavior as that of configuration 1, described above. However, in

- Time autocorrelation and Power Spectral Density (PSD)

With the aim of determining the scales of turbulence phenomena above the rooftop, analysis of time autocorrelation and PSD were conducted.

For the autocorrelation analysis, the criteria used for determining the time related to the scale of turbulence phenomenon was that corresponding to a coefficient of autocorrelation of $1/e \approx 0.37$.

According to the Taylor “frozen flow hypothesis” the scale can be calculate dby:

$$L \approx UT$$

Where L represents the scale, U the mean velocity and T the time.

Height = 5 cm	
Scale	Intersection $1/e \approx 0.37$
Time scale(s)	0.0085
Spatial scale (m)	0.02
Height = 15 cm	
Scale	Intersection $1/e \approx 0.37$
Time scale (s)	0.003
Spatial scale (m)	0.05
Height = 25 cm	
Scale	Intersection $1/e \approx 0.37$
Time scale (s)	0.1325
Spatial scale (m)	1.65

Table 1: turbulence scales in point 5 of Configuration 1

For configuration 1 it can be seen, as expected, that a height rise corresponds to an increase in the scales. Also, the difference in scales between a height of 15 cm and 25 cm is effectively important. Once again, it can be said that at 25 cm the flow pattern is that of the free stream.

Height = 5cm	
Scale	Intersection $1/e \approx 0.37$
Time scale (s)	0.01
Spatial scale (m)	0.13
Height = 15cm	
Scale	Intersection $1/e \approx 0.37$
Timescale (s)	0.045
Spatial scale (m)	0.56
Height = 25cm	
Scale	Intersection $1/e \approx 0.37$
Time scale (s)	0.3525
Spatial scale (m)	4.18

Table 2: turbulence scales in point 5 of configuration 1

The same phenomena can be seen for configuration 3. The main difference lies in the fact that scales of this configuration are higher than those of configuration 1.

There is a frequency value at which turbulence phenomena is likely to occur. The energy is concentrated near this frequency value. In order to determine this frequency, the PSD curves were calculated.

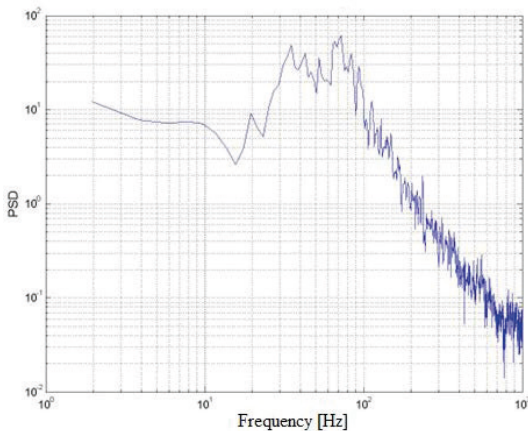


Figure N° 14: PSD at point 5 and for configuration 1.

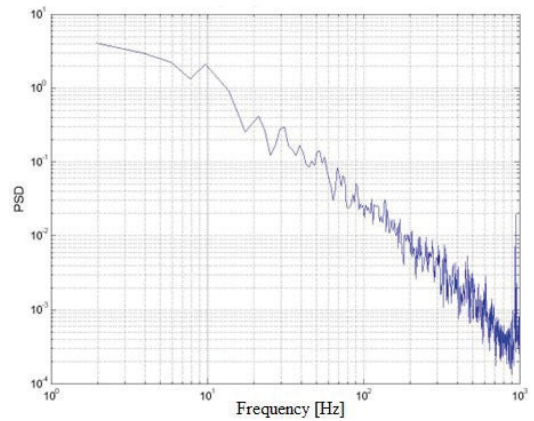


Figure 15: PSD at point 5 and for configuration 3.

For each configuration it is observed that energy concentrates at high frequencies, beginning at 500 Hz. From the PSDs, it is concluded that main turbulence phenomena occurs between 800 and 900 Hz.

CONCLUSIONS AND DISCUSSION

From the velocity field analysis, the higher velocities occurred for configurations 1 and 3. Average increases in velocity of 43% and 22% were achieved for configurations 1 and 3, respectively.

From the analysis of measurements at 9 different points above the rooftop, the variation in velocity between the planes Y1, Y2 and Y3, is less than 5%. Then, the conclusions from plane Y2 can be acceptable for planes Y1 and Y3.

It is concluded that the heights of wind turbine towers with respect to their location should be approximately:

Configuration 1

- Position 1, 2 or 3: 25 cm (20m) height – $\Delta h/h = 0.36$
- Position 4, 5 or 6: 20 cm (16m) height – $\Delta h/h = 0.29$
- Position 7, 8 or 9: 15 cm (12m) height – $\Delta h/h = 0.21$

Configuration 3

- Position 1, 2 or 3: 20 cm (16m) height – $\Delta h/h = 0.36$
- Position 4, 5 or 6: 15 cm (12m) height – $\Delta h/h = 0.21$
- Position 7, 8 or 9: 10 cm (8m) height – $\Delta h/h = 0.14$

Positions indicated on Figure 4.

h = building height

Δh = wind turbine tower height

In reference to the turbulence intensity coefficients, for configuration 1, at point 2 at 25 cm height, the coefficient is 6%. Meanwhile, for positions 5 at 20 cm height and 8 at 15 cm height it is 8% and 12 %, respectively. On the other hand, for configuration 2, the coefficient is 1.5% for each case. Therefore, these values are lower than the 18% maximum value specified by the International Standard IEC 61400-2. Furthermore, for configuration 3, even for a height of 20 cm, the coefficient is 15%, and it increases rapidly for lower heights.

It is more convenient if the building A height is much lower than that of Building B. In this way the flow above Building B is unaffected by the presence of Building A, thus an important increase in velocity can be

achieved. However, configuration 3 has some advantages. Although it has lower velocities than configuration 1, the flow is more likely to be parallel to the surface of the rooftop. This is positive in the case of using Horizontal Axis Wind Turbines (HAWTs); moreover, the turbulence intensity coefficients and rms values are lower than those of configuration 1.

The results presented above show the importance of research on the implementation of wind energy conversion in the built environment. Although several disadvantages or challenges may exist, such as the noise emission of the turbines or the risk to people, there are potential advantages such as increases in velocity and power. Thus, energy production in cities, by the use of wind, can effectively become a real solution to the increasing world wide energy demand challenge and its study should be encouraged.

REFERENCES

- [1] URBAN WIND TURBINES - GUIDELINES FOR SMALL WIND TURBINES IN THE BUILT ENVIRONMENT; February 2007; Jadranka Cace, RenCom; Emil ter Horst, HoriSun; Katerina Syngellakis, IT Power; Maite Niel, Axenne; Patrick Clement, Axenne; Renate Heppener, ARC; Eric Peirano, Ademe; Wind Energy Integration in the Urban Environment (WINEUR); [http://www.urbanwind.net/\(10/Sep/2009\)](http://www.urbanwind.net/(10/Sep/2009)).
- [2] Wang F, L. Baia, J. Fletcher, J. Whiteford, and D. Cullen; The methodology for aerodynamic study on a small domestic wind turbine with scoop; *Journal of Wind Engineering and Industrial Aerodynamics* 96 (2008) 1–24, Ed. Elsevier.
- [3] Andrew Grant, Cameron Johnstone, and Nick Kell; Urban wind energy conversion: The potential of ducted turbines; *Renewable Energy* 33 (2008) 1157–1163
- [4] Lin Lu , and Ka Yan Ip; Investigation on the feasibility and enhancement methods of wind power utilization in high-rise buildings of Hong Kong; *Renewable and Sustainable Energy Reviews* 13 (2009) 450–461.
- [5] Nalanie Mithraratne; Roof-top wind turbines for microgeneration in urban houses in New Zealand; *Energy and Buildings* 41 (2009) 1013–1018.
- [6] http://www.lanacion.com.ar/nota.asp?nota_id=908367 (14/May/2007).
- [7] Alnaser, N.W., R. Flanagan, and W.E. Alnaser; Model for calculating the sustainable building index (SBI) in the kingdom of Bahrain; *Energy and Buildings* 40 (2008) 2037–2043.
- [8] [http://www.buildinggreen.com/auth/article.cfm/2009/4/29/The-Folly-of-Building-Integrated-Wind/?sidebar=1\(10/sep/2009\)](http://www.buildinggreen.com/auth/article.cfm/2009/4/29/The-Folly-of-Building-Integrated-Wind/?sidebar=1(10/sep/2009)).
- [9] Gerald Muller, Mark F. Jentsch, and Euan Stoddart; Vertical axis resistance type wind turbines for use in buildings; *Renewable Energy* 34 (2009) 1407–1412.
- [10] [http://www.waughthistleton.com/project.php?name=ramsgate&img=1\(10/sep/2009\)](http://www.waughthistleton.com/project.php?name=ramsgate&img=1(10/sep/2009)).
- [11] Associação Brasileira de Normas Técnicas: Forças devidas ao vento em edificações- NBR- 6123/1988, Rio de Janeiro, Brasil, 1988.